Dynamics of bluff-body stabilised flames subjected to equivalence ratio oscillations

R. Balachandran[1], A.P. Dowling[2], E. Mastorakos[2]
[1] Department of Mechanical Engineering, University College London, Torrington Place,
London WC1E 7JE, UK
[2] Department of Engineering, University of Cambridge, Trumpington Street,
Cambridge CB2 1PZ, UK

Abstract

This paper describes an experimental effort to understand the dynamic response of lean premixed, bluff-body stabilised flames subjected to strong acoustic excitation resulting in time-varying equivalence ratio. The combustor has a centrally-placed bluff-body which stabilises the flame. The fuel (ethylene) was injected through six choked injectors at an upstream location to achieve a fluctuating equivalence ratio at the bluff-body plane and the resulting flame is referred here as an imperfectly premixed flame. The heat release modulation due to acoustic forcing was investigated using measurements of global heat release rates and velocity perturbations, with OH* and CH* chemiluminescence and two-microphone methods respectively. The response of these imperfectly premixed flames was found to depend on the degree to which the flame was compact acoustically and convectively. When the overall length of the flame was comparable to or greater than the wavelength of the forced oscillations (ie. high frequency forcing), the heat release modulation was dominated by flame-vortex interactions and when the flame was compact (i.e. low frequency forcing), the heat release modulation was mainly due to temporal variations in the equivalence ratio. The results presented in this paper can assist with the development of nonlinear flame models for prediction of limit cycle amplitudes in practical combustors.

Introduction

Lean premixed combustion remains as one of the most important technologies for achieving an ultra low NOx, high efficiency and low fuel economy combustion system for aero and industrial gas turbine applications. These combustion systems are found to be prone to combustion instabilities, which in many cases result in complete failure of the plant/mission [1]. Combustion instabilities in a system may arise due to combination of various mechanisms involving complex interactions between flame, acoustics, fluid mechanics and heat transfer characteristics of the system [2]. Among those, the coupling between the heat release modulation and the chamber acoustics and/or the acoustics of the fuel feed line are very common in practical devices [1, 3]. In order to predict these instabilities and to mitigate or control them, detailed understanding of the underlying physical mechanisms is essential. Intensive experimental and theoretical works [1-9] have been performed over two decades to identify different controlling mechanisms for such combustion oscillations. Continuing advancement in advanced diagnostic concepts [5, 10-11] and computational methods [12 - 13] have helped to further improve the understanding of various phenomena involved in combustion dynamics.

Various important, possible feedback mechanisms for the sustainment of combustion driven oscillations in a turbulent flame were listed by Kulsheimer [9] and also in a review by Candel [2]. Two major mechanisms which control the heat release variation in a turbulent premixed flames are (i) the flame area modulation as a consequence of flowfield-flame interaction and (ii) equivalence ratio modulation. In a recent study by Balachandran et al [5], it was showed that in a fully premixed turbulent flame (ie when there is no temporal or spatial variation in equivalence ratio) the heat release modulation was primarily due to flame area modulation. In the above study, it was shown that the flame response saturation to the imposed velocity oscillation was primarily due to strong flame-vortex interaction. The increase and decrease in flame area was shown to correspond to increased flame area due to flame rollup and the flame annihilation events respectively. There are abundant experimental data related to flow-flame interaction, primarily in laminar premixed flames, which also resulted in many theoretical models defining the laminar flame response accurately [2,6-8]. There are few studies on the role of equivalence ratio variation in combustion dynamics, both experimental and theoretical [3]. In many practical applications both the temporal variation in equivalence ratio and the velocity fluctuations occur together; hence it is important to understand the relative importance of their impact in limiting the flame response to the imposed oscillation, which is the principal motivation for this study.

This paper describes an experimental effort to understand the response of imperfectly premixed flames to strong acoustic forcing in an apparatus similar to that of Ref. [5]. The main objectives of this study were: (i) to measure and understand the non-linear response of premixed flames with time-varying equivalence ratio; (ii) to identify the mechanisms responsible for the flame response saturation and (iii) to compare the results to the measured responses of fully premixed forced flames.

---

[*] Corresponding author: r.balachandran@ucl.ac.uk

Proceedings of the European Combustion Meeting 2011

Experimental Methods

Burner

A generic laboratory scale acoustically excited bluff body combustor was used. The details of the burner setup are provided in Refs. [5,14]. For completeness, some of the details are repeated here. The burner consists of two concentric pipes, the annulus of which allows air into the combustor. The outer pipe is 450 mm long with inner diameter (*ID*) of 35 mm. A central pipe, which also houses a conical bluff body of diameter 25 mm giving a blockage ratio of 50%, stabilises the flame. The fuel (ethylene) is injected radially through six choked injectors along the circumference of the central pipe 55 mm upstream of the bluff body (see Fig.1). The outer pipe also houses pressure taps for acoustic pressure measurements. Air from the laboratory compressor enters into the combustor through a 200 mm long and *ID* 100 mm plenum chamber. To effect velocity oscillations at the bluff body, two loudspeakers were used. These speakers were mounted diametrically opposite to each other on the circumference of the plenum chamber. The loudspeakers were excited by a sinusoidal signal generated using a *TTi* 40 MHz Arbitrary waveform generator. The forcing amplitude (peak-to-peak voltage to the speakers) and the frequency of forcing were varied independently to understand the dependence of flame response on amplitude and frequency of forcing. The forcing achieved was as high as 65% of the mean velocity for certain forcing frequencies.

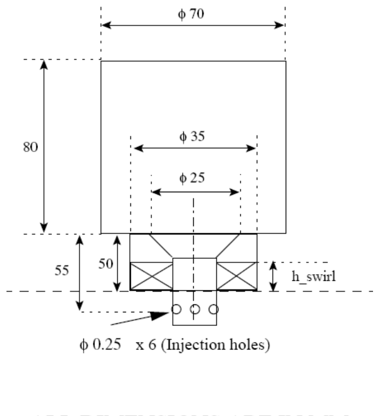

Fig. 1. A c*lose-up view of the combustor*

The flame was enclosed using a 80 mm long fused silica quartz cylinder of inner diameter 70 mm which provided optical access for the imaging and also avoided equivalence ratio (ϕ) variations due to possible air entrainment from the surroundings. For the present study, the forcing frequency was varied between 20 to 400 Hz while the fundamental frequency of the downstream duct (enclosure) is around 1000 Hz; hence the resonant effects of the downstream geometry are minimized by the selection of this short length enclosure. For all experiments, the mass flow of air at inlet to the plenum was kept constant, which was around 5 g/s (i.e., 280 lpm), resulting in a bulk velocity of 9.9m/s at the annular exit.

Measurement techniques

a. Acoustic and flow-rate measurements

The mass flow of air and the fuel were measured and controlled using BRONKHORST *Hi-Tech* mass flow controllers with measurement ranges of 12-600 litres per minute (lpm) for air and 1.2-60 lpm for ethylene, with an accuracy of ±0.5% of the Full Scale Deflection. Three Kulite high sensitivity pressure transducers (Model XCS –093 with sensitivities of $4.2857\text{x}10^{-3}$ mV/Pa) were used to measure pressure perturbations and the two-microphone technique reviewed in Ref. [15] was used to determine the bulk velocity fluctuations at the combustor inlet from the pressure measurements. The signals from the transducers were amplified, digitised and saved using a digital data acquisition system (National Instruments PCI 6034E, resolution 16 bits, input range 10 ± 0.05 V, max. sampling rate 200 kHz). Data were acquired at a sampling rate of 10 kHz and time series lasting 2 seconds were collected and stored for post-processing which resulted in a frequency resolution of 0.5 Hz. The acoustic characteristics of the combustor revealed that the burner resonant frequencies were around 40, 160 and 320 Hz and hence for the present study 40 Hz and 160 Hz are considered.

b. Heat release measurements

Chemiluminescence emission from the flame (OH* and CH*) were recorded to quantify the heat release modulation. Details and applicability of these techniques for flame response studies are found in Refs. [5,11]. The global OH* and CH* chemiluminescence was measured with Hamamatsu (R3788) side-on PMTs, both fitted with interference filters of 10 nm bandwidth centred at 307 nm and 435 nm respectively. The signal collection optics used for OH*/CH* chemiluminescence measurement were designed to collect light from the entire combustion zone. During the current work, along with the PMT measurements, the OH* chemiluminescence was also recorded simultaneously by using an Intensified CCD camera, for which the intensifier was gated at 50μs. The collection wavelength of OH* chemiluminescence images was broader for the imaging (from 305 nm to 400 nm). The flame dynamics was further investigated for some of the cases presented here using OH Planar laser induced fluorescence. The OH PLIF images were then processed to obtain flame surface density (*FSD*). The details of the measurement method are provided in Ref. [5].

c. Fuel concentration measurements

In order to understand the effect of acoustic forcing on the temporal variation of equivalence ratio, the fuel concentration was measured using a CAMBUSTION HFR500 fast Flame Ionisation Detector (*FID*) with a 1-mm-diameter sampling probe. The detector had a response time of about 0.9 ms, and a sample gas flow rate of about 0.5 L/min. The probe was placed at the bluff body plane in the center of the annular flow passage. These experiments were carried out in the absence of flame. The signal of the *FID* device was recorded along with the reference forcing signal to eventually correlate the fuel concentration data with the heat release measurements. The phase lag between the reference and the *FID* signal were found to be about 10 ms. The fuel concentration measurements were used to evaluate the equivalence ratio variations.

Determination of the flame response

The time traces of OH* and CH* were analysed spectrally for different forcing frequencies and amplitudes using the Fast Fourier transform (FFT) technique and used to evaluate the flame transfer function H, a quantity commonly employed to measure the response of flame to acoustic forcing. If the instantaneous flow velocity at the burner exit is U, then $U(t)= \langle U\rangle + u'(t)$, where "$\langle\rangle$" and primes represent the mean and the fluctuating components, respectively. Similarly, if Q is the heat release rate, $Q(t)= \langle Q\rangle + Q'(t)$. The non-linear flame transfer function or non-linear frequency response function can then be defined as $H(f,A)$:

$$H(f,A) = [Q'(f)/\langle Q\rangle] / [u'(f)/\langle U\rangle]. \qquad - (1)$$

where, $\langle Q\rangle$ is the time-averaged heat release rate, $\langle U\rangle$ is the bulk velocity of the mixture entering the combustor, Q' and u' are their corresponding half peak-to-peak amplitudes at frequency f (i.e. the amplitudes of the Fourier transforms of Q and U, narrow-band filtered around f) and A is the magnitude of $u'(f)/\langle U\rangle$ (i.e. ratio of half peak-to-peak amplitude of velocity oscillation at harmonic forcing frequency f to the bulk velocity).

From power spectra, the complex amplitude of the quantities OH*' and CH*' at the forcing frequency f, were determined. These values were normalised using the time mean values of OH* and CH* respectively to obtain $OH^{*\prime}(f)/\langle OH^*\rangle$ and $CH^{*\prime}(f)/\langle CH^*\rangle$ which are used as estimates of $Q'(f)/\langle Q\rangle$. The two quantities $Q'(f)/\langle Q\rangle$ and $u'(f)/\langle U\rangle$ determined from the simultaneous acoustic pressure measurements using the two-microphone method to estimate $H(f,A)$ in Equation 1.

Results and Discussion

Figure 2(a) shows the dependence of the OH* and CH* chemiluminescence upon the inlet forcing amplitude at a particular forcing frequency, 160 Hz. Figure 2(b) shows the magnitude of the transfer function H and the corresponding phase information calculated from the data presented in Fig. 2(a). The results suggest that at this forcing frequency, the flame response was linearly dependent on the acoustic forcing amplitude A. It can be seen from Fig. 2(b) that the phase of the transfer function was nearly independent of the amplitude of forcing. From these results it is also clearly evident that the magnitude and phase of the heat release response measured by both the OH* and CH* chemiluminescence techniques are in good agreement as in the case of fully premixed flames presented in Ref. [5].

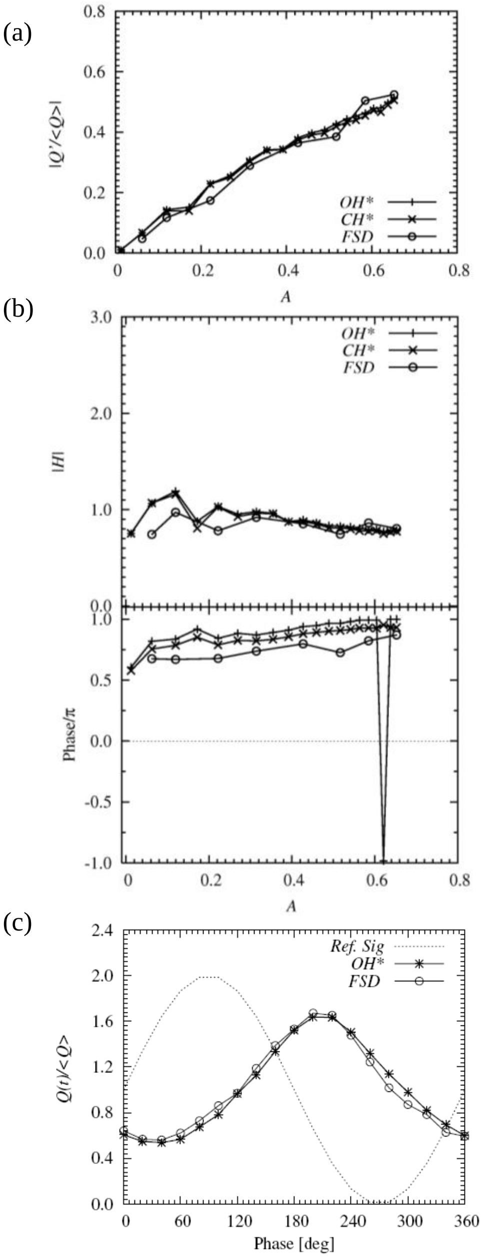

Fig. 2. (a) The normalised global heat release fluctuation of flame. (b) The corresponding transfer function and the phase. (c) Comparison of heat release variation from FSD and OH* data at A=0.65: f=160 Hz, $\langle U\rangle$ =9.9 m/s, global ϕ = 0.55.

The heat release response evaluated from *FSD* as a function of forcing amplitude is the same as that of

OH* and CH* measurements (see Fig. 2(b)). These measurements suggest that for this flame the level of contribution from flame surface modulation towards the total heat release response is significant and the flame area evolution is playing a key role in the observed amplitude dependence. The direct effect of the variation in burning speeds due to time-varying equivalence ratio does not seem to be significant for this flame at the reported forcing condition. The agreement between the magnitude and phase of heat release modulation evaluated from *FSD* and OH* presented in Fig. 2(c), and the transfer function data from different techniques presented in Fig. 2(b), confirms the above conclusion, i.e. that the flame surface modulation controls the heat release rate modulation in this flame. Figure 3 shows the equivalence ratio fluctuation measured for the highest forcing amplitude condition at this frequency. It can be clearly seen from this figure that the variation in equivalence above the mean is relatively small. These results support the inferences made earlier using *FSD* and OH* data.

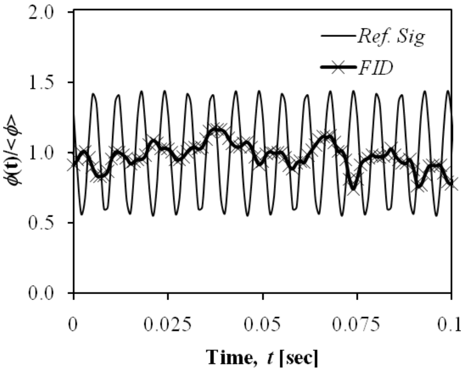

Fig. 3. The normalised equivalence ratio fluctuation obtained from FID measurements. *f*=160 Hz, *A*=0.65, $\langle U \rangle$ =9.9 m/s, global ϕ = 0.55.

The finite amplitude response of the imperfectly premixed flame was also investigated at low frequency forcing. Figure 4 shows the amplitude dependence of heat release response of the flame at 40 Hz with the corresponding magnitude of transfer function and the phase information measured using OH* and CH* chemiluminescence. The figure suggests a highly nonlinear amplitude dependence. The magnitude of the transfer function presented in Fig 4(b) also suggests a very high response, which is at the least two to three times higher than the magnitude of the response at 160 Hz. The phase of the transfer function measured seems to be linearly dependent on the amplitude.

The time-series of OH* chemiluminescence for high forcing amplitude (from the data used for Fig. 4) is presented in Fig. 5. The OH* chemiluminescence data was normalized using the time-mean of the signal and the reference signal was scaled (by a factor of 2) and offset (by a value of 1.0) for better presentation. It can be seen clearly that the increase in the heat release was much steeper than the decay of the signal. With an increase in amplitude, the region of the heat release cycle with low values reached values close to zero. However, it should be noted that the values did not reach zero in any part of the cycle. For comparison with the fully premixed flame response at 40 Hz, the time-series at the highest amplitude is presented in Fig. 5(b). It can be seen clearly from these figures and from previous work [5] that the flame response at 40 Hz for imperfectly premixed was much greater (by a factor of 2) compared to the fully premixed flame response. The cold flow smoke visualization and FSD measurements at this forcing condition, provided in Ref. [14], suggested that there was no shear layer roll up, however the characteristic length and width of the recirculation varied significantly with phase. The response of the fully premixed flame presented in Ref. [5] also suggested a linear dependence for forcing at 40 Hz, contrary to the evidence in Fig. 4(a).

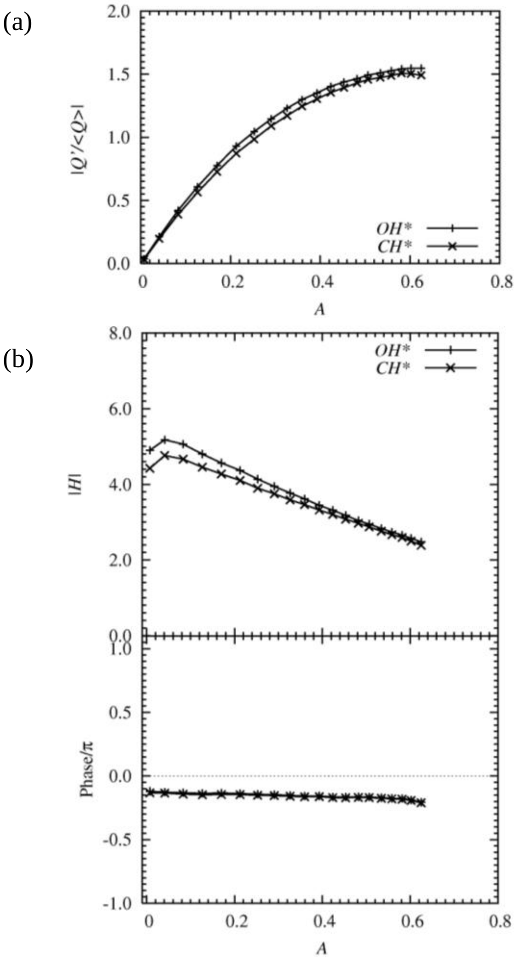

Fig. 4. (a) The normalised global heat release fluctuation of flame. (b) The corresponding transfer function and the phase: *f*=40 Hz, $\langle U \rangle$ =9.9 m/s, global ϕ = 0.55.

These results suggest that for forcing frequency at 40 Hz, the response was not dominated by the flame surface modulation due to flame-vortex interaction. It can be speculated that the steep increase in heat release values and the values approaching zero could be due to variation in the equivalence ratio. The low values in heat release rates could be due to the fact that the oscillation in equivalence ratio could have resulted in mixture concentration close to the extinction limits locally or even globally, resulting in much decreased heat release. At 40 Hz forcing and for bulk velocity of 9.9 m/s, the flame enclosed in a 80 mm long tube is very compact acoustically-convectively, meaning the effect of cycle variation in equivalence ratio would affect greatly the global equivalence ratio and thus the heat release. In order to evaluate the above inferences, the *FID* measurements for the above condition are presented in Fig 6. The data is presented for the highest forcing condition. It can be clearly seen from the figure that the equivalence ratio varied significantly through the cycle and for about half of the cycle the equivalence ratio value was well below the mean value, which agrees well with the OH* time-series data presented in Fig. 5.

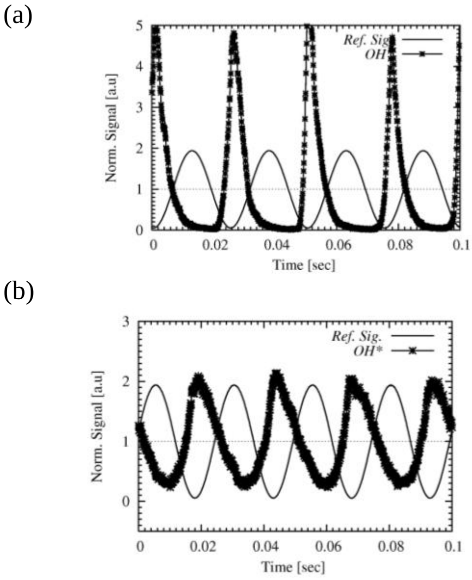

Fig. 5. Time-series of simultaneously measured reference signal and OH* data from (a) imperfectly premixed (A=0.63) and (b) fully premixed (A=0.64) flames. f=40 Hz, $\langle U\rangle$ =9.9 m/s, global ϕ = 0.55.

The phase-averaged images of OH* was used to further evaluate the flame shape. The flame response evaluated from these images (see Chapter 5 in Ref [14]) confirmed the response evaluated from PMT measurements. From these images, it was also observed that there was no vortex roll up, suggesting that the variation in heat release could be mainly due to variation in equivalence ratio. It should be noted here that the flame did not blow out completely during the cycle. The instantaneous OH* images suggested the presence of isolated flame regions. The results suggest that the heat release remained non-zero throughout the cycle.

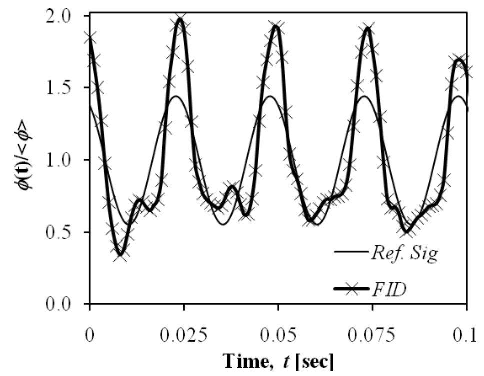

Fig. 6. The normalised equivalence ratio fluctuation obtained from FID measurements: f=40 Hz, A=0.63, $\langle U\rangle$ =9.9 m/s, global ϕ = 0.55.

The results presented in this work suggest that the flame response of imperfectly premixed flames is controlled by two mechanisms, based on whether the flame is acoustically-convectively compact or not. When the flame was compact (i.e. f was low) the heat release modulations were highly nonlinear and the saturation mechanism was dominated by equivalence ratio modulation. When the flame was not acoustically-convectively compact (i.e. f was high), the flame response was dominated by the flame area modulation due to the vortex roll up.

Frequency Scaling

In order to understand the relative importance of the two mechanisms described above from the various measurements performed, the frequency of forcing was normalized using the fuel convection time, and the transfer function as a function of this normalized frequency for various conditions was consolidated in Fig. 7. The convection time for a non-swirling flame was obtained by dividing the length of the flame (L_f) with the bulk velocity ($\langle U\rangle$). This value was used to normalize the forcing frequency to obtain the reduced frequency. Figure 7 contains the measured response of fully premixed and imperfectly premixed flames. The figure suggests that the magnitude of response of imperfectly premixed flames were high compared to the fully premixed cases (by factor of 3), when the flame was compact (i.e. when the value of reduced frequency was much less than 1). The response of the flame decreased (magnitude of H decreased) with increase in the reduced frequency, i.e. with decrease in compactness. The H values for fully premixed flames and imperfectly premixed flames are of comparable magnitude for reduced frequency values close to one and above, where the acoustic wavelengths are comparable to the flame lengths. This suggests that during low frequency forcing, the change in equivalence ratio at the flame front could be felt globally affecting the heat release, while during the high frequency forcing these effects are not comparable to the flame kinematic contributions from vortex-flame interaction. The balance of these two mechanisms and the phase between them could be playing an important role in the nonlinear frequency response of the flames. The transfer function values reaching values close to zero for certain frequencies in between these two frequencies could be because the two mechanisms are balancing each other. The role of these two mechanisms did not change even when the flow was swirled (see Ref. [14]).

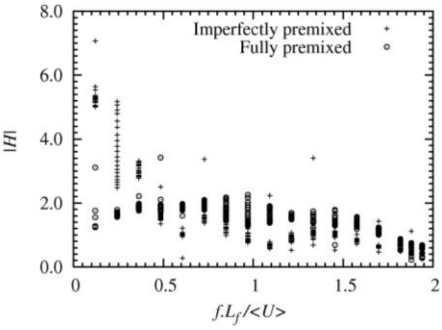

Fig. 7. Comparison of the magnitude of transfer functions of imperfectly premixed and fully premixed flames as a function of reduced frequency. $\langle U \rangle$ =9.9 m/s, global ϕ = 0.55.

Conclusions

This work describes an experimental effort to understand to the response of imperfectly premixed flames subjected to strong acoustic forcing in a model bluff-body combustor, where the partial premixing (imperfectness) was achieved by injecting fuel (ethylene) through six choked injectors upstream of the bluff body. The global heat release rates were measured with OH* and CH* chemiluminescence.

The results presented here show that the heat release response in imperfectly premixed flames has contributions through two mechanisms: equivalence ratio fluctuations and flame area modulation due to strong flame-vortex interaction. The former dominates the saturation mechanism of the flame response when the flame is compact and the latter plays a significant role when the acoustic wavelengths and the flame length are of comparable magnitude.

Acknowledgements

The authors would like to thank EPSRC, DTI, and Rolls Royce plc for the funding. The authors would also like to thank Dr SF Ahmed, King Fahd University, Saudi Arabia for his help with the FID measurements.

References

1. A. P. Dowling, *Aeronautical Journal* 104 (2000) 105-116.
2. S. Candel, *Proc. Comb. Inst.* 29 (2002) 1-28
3. A.P. Dowling, S.R. Stow, *J. Prop. Power* 19 (2003) 751-764.
4. T. Lieuwen, *J. Prop. Power* 19 (2003) 765-781.
5. R. Balachandran, B.O. Ayoola, C. F. Kaminski, A. P. Dowling , E. Mastorkatos, *Combust. Flame* 143 (2005) 37-55..
6. F. Baillot, D. Durox, R. Prudhomme, *Combust. Flame* 88 (1992) 149-168.
7. S. Ducruix, D. Durox , S. Candel, *Proc. Combust. Inst.* 28 (2000) 765-773.
8. T. Schuller, D. Durox, S. Candel, *Combust. Flame* 134 (2003) 21-34.
9. C. Kulsheimer and H. Buchner, *Combust. Flame* 131 (2002) 70-84.
10. J.G. Lee, D.A. Santavicca, *J. Prop. Power* 19 (2003) 735-750.
11. D. Veynante, J. M. Duglos, J. Piana , *Proc. Comb. Inst.* 25 (1994) 1249-1256.
12. T. Poinsot, S. Candel, A Trouve, *Prog. Energy Combust. Sci*. 21 (1995) 531-576.
13. C. A. Armitage, R. Balachandran, E. Mastorakos, R. S. Cant *Combust. Flame* 146 (2006) 419-436.
14. R. Balachandran, PhD Thesis, *University of Cambridge* (2005).
15. A.F. Seybert, D.F. Ross, *J. Acoust. Soc. Am.* 61 (1977) 1362-1370